Analysis Method for the Heating of the Human Eye Exposed to High Frequency Electromagnetic Fields

Hrvoje Dodig, Andrés Peratta and Dragan Poljak

Original scientific paper

Abstract: **The paper studies the thermal rise in the human eye caused by time harmonic electromagnetic waves. An eye has been illuminated by a high frequency plane wave with power density 5.0 mW/cm^2. Such a problem has been considered as an electromagnetic scattering problem since part of EM energy is transmitted to the eye and part of it is reflected. The total electric field inside an eye and related Specific Absorption Rate (SAR) has been calculated in a frequency range from 0.7 to 4.4 GHz via a hybrid BEM/FEM approach. Knowing the SAR distribution inside the eye provides the calculation of related temperature rise in the human eye due to high frequency radiation by solving Bio-Heat Transfer Equation via standard finite element method.**

***Index terms*: hybrid BEM/FEM, electromagnetic heating, Specific Absorption Rate, Bio-Heat Transfer Equation**

I. INTRODUCTION

In the last decade there has been an increasing interest regarding the influence of high frequency electromagnetic fields produced by modern microwave devices, such as cellular phones or WLAN devices, on human health [1]-[3].

It is well known that temperature rise is predominant effect when the human tissue is exposed to high frequency (HF) electromagnetic fields [4]. This temperature rise is directly related to specific absorption rate (SAR) which is proportional to the squared value of the electric field. Therefore, it is necessary to calculate the electric field distribution inside the tissue in order to determine the corresponding thermal rise.

This paper deals with the thermal rise in the human eye caused by high frequency radiation. The eye is investigated primarily due to the fact that it is not protected by layer of skin and bones thus making it the most vulnerable organ to electromagnetic radiation, as well.

The heating of the human eye due to the absorbed energy from radiation is regarded as an electromagnetic scattering problem. The human eye is irradiated by HF external field and part of EM energy is transmitted to the eye and part of it is reflected from the eye. The backscattered field must be allowed to propagate towards the infinity otherwise multiple reflections from the artificial (computational) boundary of the problem can occur.

Manuscript received December 2, 2005 and revised September 5, 2006.
Hrvoje Dodig and Andrés Peratta are both with the Wessex Institute of Technology, Ashurst Lodge, Southampton, UK

Dragan Poljak is with the Department of Electronics, Faculty of Electrical Engineering, University of Split, Croatia (e-mail: dpoljak@fesb.hr).

Numerous techniques may be used in order to calculate the electric field distribution inside the tissues; i.e. Finite Difference Time Domain (FDTD), Finite element Method (FEM) [3],[5], and Boundary Element Method (BEM), [4],[5]. Each of these methods has distinct advantages and disadvantages. FDTD is one of the simplest techniques and most commonly used. FEM can be used in conjunction with various absorbing boundary conditions in order to allow the reflected electromagnetic energy to propagate towards the infinity. BEM is an excellent technique for solving scattering problems in electromagnetism since it tolerates cropping the physical domain of the model without creating artificial reflections at the boundaries but it generates fully populated matrices and does not handle in easy way non-homogeneous material properties such as occurs in the human eye. In this paper, the hybrid technique featuring advantages of both BEM and FEM is used to obtain electric field distribution inside an eye.

Once the electric field distribution inside the eye is available one may proceed with the SAR computation. Finally, the temperature rise in the human eye can be obtained using the SAR as input parameter in the Bio-Heat transfer equation which is solved with a standard FEM procedure.

II. ELECTROMAGNETIC MODELING OF THE HUMAN EYE

Fig. 1 shows the schematic representation of the electromagnetic scattering problem. The scatterer inside computational domain Ω is considered inhomogeneous and it represents the part of the human head illuminated by time harmonic, HF plane wave. Thus, an eye is considered as a part of the scatterer.

The incident wave is considered to be a time harmonic with arbitrary direction and having either TM or TE polarization. This incident electric $\vec{E}_z^{inc}$ or magnetic $\vec{H}_z^{inc}$ field can be described, for TM and TE mode, respectively, as

$$\vec{H}_z^{inc} = \vec{e}_z H_0^{inc} e^{j\vec{k}\cdot\vec{r}} \quad (1)$$

$$\vec{E}_z^{inc} = \vec{e}_z E_0^{inc} e^{j\vec{k}\cdot\vec{r}} \quad (2)$$

In order to determine electromagnetic fields inside the computational domain Ω the Helmholtz equations for electric and magnetic fields need to be solved.

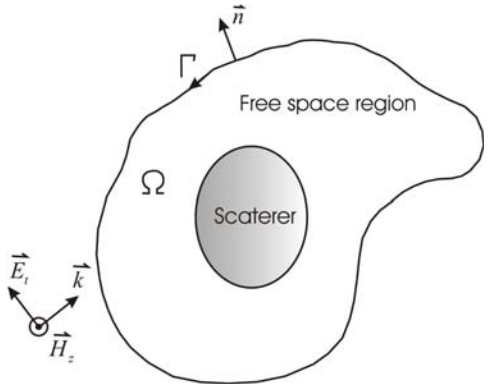

Fig. 1. Schematic representation of EM scattering problem. In this figure time harmonic EM wave in TM mode is incident on the boundary Γ of the computational domain Ω. Vector $\vec{n}$ is outward normal to the bounding curve Γ. The scatterer is considered as inhomogeneous region while the space around the scatterer is considered as homogeneous region.

A. Governing Equations

For EM scattering problems FEM must be used with some kind of boundary conditions. This can be absorbing boundary conditions (ABC) or perfectly matched layer (PML). In this paper, however, the necessary boundary condition is obtained from BEM. This might be more accurate since ABC's and PML's are only approximations while BEM terminates the computational domain mathematically correctly.

The hybrid BEM/FEM takes advantage of both BEM and FEM features in order to simplify the procedure for solving electromagnetic scattering problems that involve inhomogeneous objects. The governing differential equations for FEM can be readily derived from Maxwell equations yielding [6]:

$$\nabla\times\left(\frac{1}{\omega\mu}\nabla\times\vec{E}\right)+\left(j\sigma-\omega\varepsilon\right)\vec{E}=0 \tag{3}$$

$$\nabla\times\left(\frac{1}{\sigma+j\omega\varepsilon}\nabla\times\vec{H}\right)+j\omega\mu\vec{H}=0 \tag{4}$$

By manipulating Maxwell's equations directly and by using the following constitutive relationships:

$$\vec{J}=\sigma\vec{E} \tag{5}$$

$$\vec{D}=\varepsilon\vec{E} \tag{6}$$

where $\vec{J}$ denotes the conductive current and electric flux density, respectively, one obtains [6]:

$$\nabla^2\vec{E}+k^2\vec{E}=\frac{1}{\varepsilon}\nabla\rho+j\omega\mu\vec{J}=-\vec{f}_E(\vec{r}) \tag{7}$$

$$\nabla^2\vec{H}+k^2\vec{H}=-\nabla\times\vec{J}=-\vec{f}_M(\vec{r}) \tag{8}$$

which are more suitable for BEM-based formulations.

In equations (7) and (8) $\vec{f}_E$ and $\vec{f}_M$ are considered spatially dependent source terms for electric and magnetic field, respectively. If there were no inhomogeneous scatterer inside Ω equations (7) and (8) would reduce to ordinary Helmholtz equations in case of free propagation without inhomogeneous terms, since in that case $\vec{f}_E=\vec{f}_M=0$.

B. Boundary Integral Equations

The general three-dimensional electromagnetic scattering problem is shown in Fig. 1. The Boundary Integral Equation (BIE) formulation applied to surface S' is needed in order to couple FEM with BEM. The BIE formulation can be derived by using the second Green's theorem [6] and the electric and magnetic fields can be expressed as:

$$E_z(\vec{r})=E_z^{inc}(\vec{r})+\iint_{S'}\left[E_z\frac{\partial G(\vec{r},\vec{r}')}{\partial n}-G(\vec{r},\vec{r}')\frac{\partial E_z}{\partial n}\right]dS' \tag{9}$$

$$H_z(\vec{r})=H_z^{inc}(\vec{r})+\iint_{S'}\left[H_z\frac{\partial G(\vec{r},\vec{r}')}{\partial n}-G(\vec{r},\vec{r}')\frac{\partial H_z}{\partial n}\right]dS' \tag{10}$$

where E_z and H_z are total electric and magnetic fields, E_z^{inc} and H_z^{inc} are incident electric and magnetic field, and the terms involving the surface integrals can be regarded as scattered electric and magnetic fields, respectively.

For 2D scattering problems volume Ω becomes surface and Γ becomes the curve bounding that surface (see Fig. 1) so that equations (9) and (10) become:

$$E_z(\vec{r})=E_z^{inc}(\vec{r})+\int_{\Gamma}\left[E_z\frac{\partial G(\vec{r},\vec{r}')}{\partial n}-G(\vec{r},\vec{r}')\frac{\partial E_z}{\partial n}\right]d\Gamma \tag{11}$$

$$H_z(\vec{r})=H_z^{inc}(\vec{r})+\int_{\Gamma}\left[H_z\frac{\partial G(\vec{r},\vec{r}')}{\partial n}-G(\vec{r},\vec{r}')\frac{\partial H_z}{\partial n}\right]d\Gamma \tag{12}$$

The Green's function for the two-dimensional case is expressed as [5],[6]:

$$G(\vec{r},\vec{r}')=\frac{j}{4}H_0^{(2)}(k|\vec{r}-\vec{r}'|)=\frac{j}{4}H_0^{(2)}(kR) \tag{13}$$

where $H_0^{(2)}$ is Hankel's function of zero order and second kind while $R=|\vec{r}-\vec{r}'|$.

C. BEM/FEM Discretization

After the BIE for EM scattering problems are established the computational domain is discretized as shown in Fig. 2. The boundary of the problem (Γ) is discretized into a finite number of linear discontinuous elements [7], as shown in Fig. 3, where both values of the field and its normal derivative

vary linearly over the segment.

The full mathematical description of the BEM/FEM hybrid approach can be found in [5].

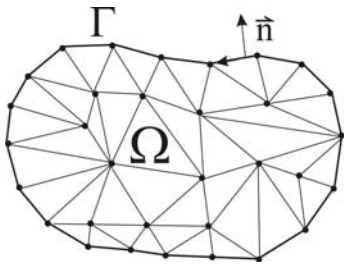

Fig. 2. Discretization scheme for BEM and FEM. Computational domain Ω is discretized into isoperimetric triangles while computational boundary Γ is discretized into linear isoparametric discontinuous elements.

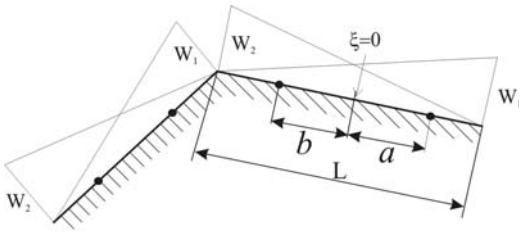

Fig. 3. Discontinuous boundary element. The collocation nodes are shifted towards the interior of the element. In the above figure, *L* is the length of the element, *a* and *b* are distances (given in local coordinates of the element) of the collocation nodes from the center of the element.

D. Boundary Conditions with Hybrid BEM/FEM

This section describes the underlying fundaments of the boundary conditions used in the hybrid BEM/FEM. Basically, the interior region is treated with the FEM, whereas the exterior region is treated with BEM. The two methods are coupled by enforcing continuity matching conditions of tangential magnetic and electric field on the boundary Γ. This can be expressed in terms of the following two equations:

$$\vec{n} \times \vec{H}^{ext} = \vec{n} \times \vec{H}^{int} \tag{14}$$

$$\vec{n} \times \vec{E}^{ext} = \vec{n} \times \vec{E}^{int} \tag{15}$$

Note that if the incident wave is in TM mode the it results convenient to formulate the problem in terms of H_z component while if the incident field is in TE mode, then the E_z component plays a more protagonist role in the method. This is owing to the fact that the problem sketched in Fig.4 is two dimensional, and because of above mentioned arguments, the boundary conditions for TM and TE mode can be written as:

$$H_z^{ext} = H_z^{int} \tag{16}$$

$$E_z^{ext} = E_z^{int} \tag{17}$$

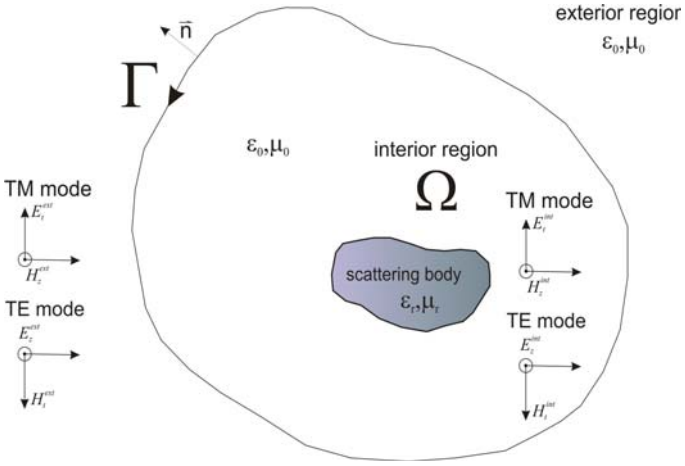

Fig. 4. General schematics of all scattering problems in this paper. Interior region Ω is considered as computational domain. Region Ω is bounded by curve Γ. Incident field is plane wave either in TE or TE mode.

III. SAR COMPUTATION

The Specific Absorption Rate (SAR) represents the mass averaged rate of energy absorption in body tissue [4],[8], given by:

$$SAR = \frac{d}{dt}\frac{dW}{dm} = \frac{d}{dt}\frac{dW}{\rho dV} \tag{18}$$

When exposed to time varying EM fields, the total power dissipated inside the human body can be determined from its current distribution [9] by mean of the following formula:

$$P = \int_V \frac{1}{2}\vec{E} \cdot \vec{J}^* dV \tag{19}$$

where $\vec{J}^*$ denotes the complex conjugate of current density. Then from the Ohm's law $\vec{J}^* = \sigma \vec{E}^*$; it follows that

$$P = \frac{1}{2}\int_V \sigma \vec{E} \cdot \vec{E}^* dV \tag{20}$$

Then, the local SAR at any point in the tissue can be expressed as:

$$SAR = \frac{1}{\rho}\frac{d}{dt}\frac{dW}{dV} = \frac{\sigma}{2\rho}\vec{E} \cdot \vec{E}^* \tag{21}$$

where σ is the electric conductivity of the tissue, ρ is the mass density and $\vec{E}$ and $\vec{E}^*$ are the electric field and its complex conjugate field, respectively.

IV. Thermal Rise in the Human Eye due to Electromagnetic Radiation

The heat transfer phenomena in biological tissue can be analyzed by solving the bio-heat transfer equation derived by Harry H. Pennes [10]. Originally, this equation has been derived to describe the thermal transport in the human forearm and it has been later modified with an additional source term that accounts for electromagnetic-related heat production, e.g. [1],[2],[4]. Next, the Bio-Heat transfer equation is usually written in the following form [4]:

$$\rho C \frac{\partial T}{\partial t} = \nabla \cdot (k \nabla T) + Q_b + Q_m + Q_{EM} \tag{22}$$

where Q_b is the term associated with blood perfusion, Q_m represents the metabolic heat generation and Q_{EM} is the new term which accounts for heat generated by EM fields. The electromagnetics term, Q_{EM}, can be expressed in terms of specific absorption rate (SAR) and mass density (ρ) as

$$Q_{EM} = \rho SAR \tag{23}$$

Heat generation due metabolic activity is always present in biological tissues and it is responsible for keeping blood temperature constant, at approximately 37°C. The effects of arterial blood supply, which denotes the rate of heating or cooling by arterial blood flow can be expressed as [4]:

$$Q_b = W_b C_{pb} (T_a - T) \tag{24}$$

where W_b is the volumetric blood perfusion rate for particular tissue, C_{pb} is the specific heat of blood and T_a is the arterial temperature which is considered to be T_a =37°C . This can be written in more compact form as

$$Q_b = B(T_a - T) \tag{25}$$

This paper considers the temperature distribution in steady conditions, that is when the thermal equilibrium has been established, after a characteristic transient time (τ_d) of typically:

$$\tau_d \approx \frac{\rho C}{k} \Delta x^2 \tag{26}$$

where, $\Delta x \approx 25mm$, is the characteristic length scale of the eye. A reasonable estimation gives $\tau_d \approx 40s$, after when equation (22) may be simplified to:

$$\nabla \cdot (k \nabla T) + B(T_a - T) + Q_m + \rho SAR = 0 \tag{27}$$

The heat transfer problem is closed with the addition of proper boundary conditions. In this case the suitable choice is to consider a mixed (or convective) condition such as:

$$k \frac{\partial T}{\partial n} = -h_c (T - T_e) \tag{28}$$

where k is thermal conductivity of the medium at the computational boundary of the problem, h_c is the heat transfer coefficient and T_e is the ambient temperature.

The solution of the problem defined by eqs (27) and (28) has been obtained by mean of standard FEM. An outline of the FEM procedures for bio-heat transfer equation can be found in [5] or [11].

V. Numerical Results

A. Test Examples

The hybrid BEM/FEM method was tested on numerous examples [5] in order to prove its performance and reliability.

In the first example the proposed hybrid method (HEM) is used to numerically calculate the focal length of the converging lens. From geometrical optics, the focal length can be expressed by the analytical equation [12]:

$$f = \left| \frac{R}{\eta - 1} \right| \tag{29}$$

where R is the radius of curvature of the lens and η is the refraction index. Results obtained for this example are in good agreement with analytic solution for focal length, resulting in focal length being calculated numerically as f = 3cm, as shown in Fig. 5.

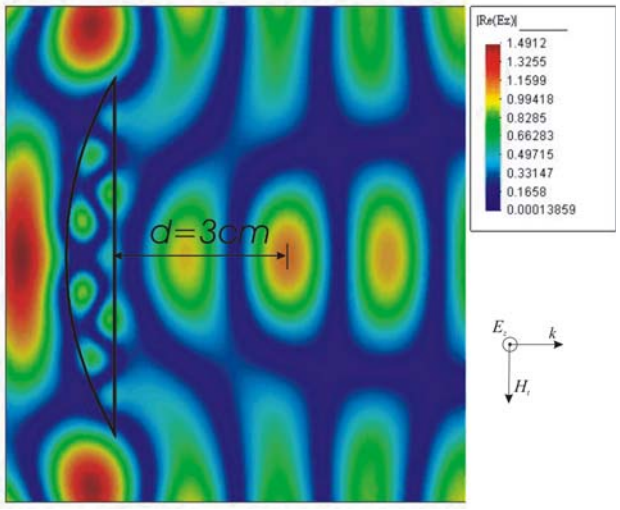

Fig. 5. TE plane wave incident on converging lens with R=6cm and refraction index η=3 is focused to a spot 3 cm away. Plane wave amplitude used in calculation was E_{z0}=1V/m and wavelength λ=3cm. Mesh consisted of 5748 triangular elements and contained 2969 nodes. Artificial boundary was modeled with 188 boundary elements.

A second example considers the problem of semi-infinite metallic surface exposed to a plane EM wave. The integration domain is shown in Fig. 6. The metal used in calculation

corresponds to the alloy MHP101 characterized by an electric conductivity of σ=17 S/m.

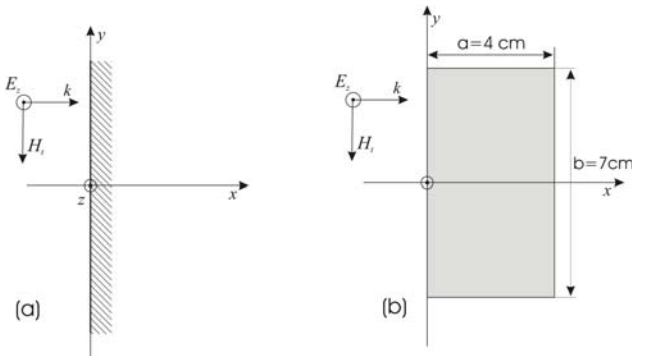

Fig. 6. Plane wave with electric field component along z axis incident on infinite metallic surface is shown in (a). On the right hand side (b) is the model used with hybrid BEM/FEM method. Electric field component is calculated along positive x axis.

The incident field is parallel to z direction, and the propagation vector is in x direction. The relative magnitude of the electric field along x axis in the infinite metallic surface equation is given by [7]:

$$\frac{|E_z|}{|E_{z0}|} = e^{-x\sqrt{\frac{\omega\mu\sigma}{2}}} \tag{30}$$

where $|E_{z0}|$ is the absolute value of magnitude of electric field at point $x = 0$. The skin depth, representing the distance for which $|E_{z0}|$ vanishes to $1/e$ of its initial value is expressed as:

$$\delta = \sqrt{\frac{2}{\omega\mu\sigma}} \tag{31}$$

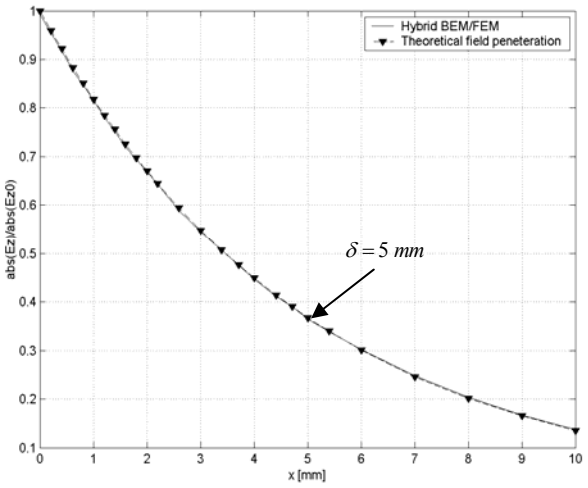

Fig. 7. Theoretical values of plane wave penetration in the metallic block are compared with values obtained by hybrid BEM/FEM method. Frequency of the plane wave was f=0.596 GHz and material was alloy MHP101 with conductivity σ=17 S/m. Value δ=5 mm represents the skin depth.

Skin depth was calculated theoretically using equation (31) and it turned out to be δ=5 mm for frequency of f=0.596 GHz and conductivity of material σ=17 S/m. The result from the numerical calculation is in very good agreement as shown in Fig. 7.

B. Electromagnetic Response of the Eye

The geometry of the human eye and its surrounding tissues used in this work was obtained from MRI images and CT scans. This data is publicly available from ref. [13] and it is anatomically-detailed three dimensional representation of the normal male and female human body.

Part of the human head was added to the calculation, as shown in Fig. 8. The reasons for adding it are: first, the conductivity of the tissues rises with frequency and second the electric field penetration into the tissue decreases with conductivity and frequency as outlined by equation (30).

Therefore, it is reasonable to conclude that backscattered fields from the back of the skull would affect the eye very lightly when HF fields are considered. However, the nose is included in the calculation due to the fact that it represents a sharp semi-conductive object and then high electric field values could be expected around the tip of the nose.

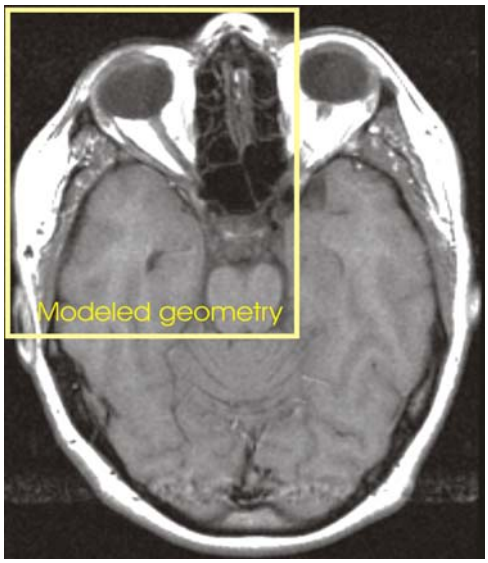

Fig. 8. The part of the head used in the calculation of thermal rise caused by EM radiation. MRI image is obtained from ref. [13].

It is common practice to describe the variation of electric permittivity and conductivity with frequency by means of 4-Cole Cole extrapolation [14]. Such an approximation is well tested in-vivo measurements on humans [15]. The electrical properties of the human eye are shown in Fig 9. and 10.

Electrical properties of tissues involved in electric field distribution calculation were not obtainable for every tissue that comprises an eye. Where these properties were not available, they were estimated with properties of blood or muscles depending on function of the tissue.

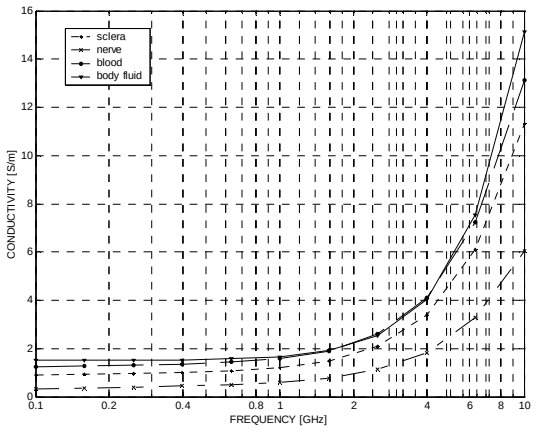

Fig. 9. The conductivity rise of various eye tissues with frequency in the frequency range from 100 MHz to 10 GHz.

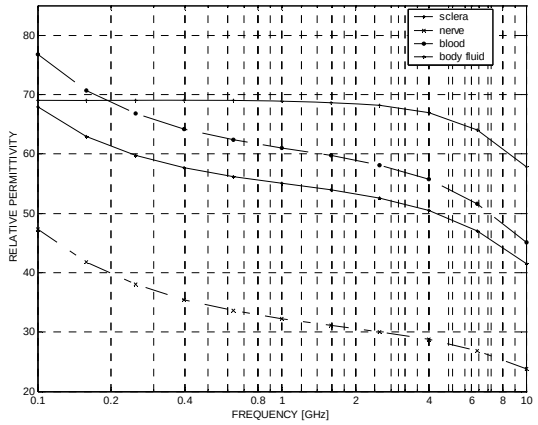

Fig. 10. The permittivity drop of various eye tissues with frequency in the frequency range from 100 MHz to 10 GHz.

Numerical results of the electromagnetic stage of the calculation are shown in Figures 11 and 12. The electric field and SAR distribution for both TE and TM polarization were obtained for left eye, in the frequency range between 0.7GHz and 4.4GHz for an input power of $5.0 mW/cm^2$.

The distribution of total electric field induced inside the eye and its close vicinity is shown in Fig. 11, while the corresponding SAR in the eye is presented in Fig 12.

It can be observed that in Fig. 12 that high values of SAR appear close to the retina. However, this is a local effect. Eye averaged SAR results are more representative of global absorption properties. The corresponding results for the whole-eye averaged SAR are shown in Figure 13. The results obtained with the Hybrid BEM/FEM were compared to those found in previous investigations conducted by Akimata et al [16], with which good agreement has been observed. Figure 14 cites the eye-averaged SAR results obtained in [16], from FDTD calculations.

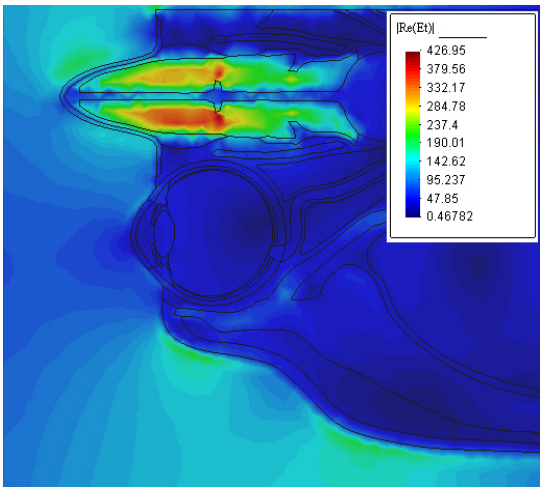

Fig. 11. The electric field distribution expressed in [V/M] caused by incident TM plane wave at frequency of 0.85 GHz as solved by hybrid BEM/FEM

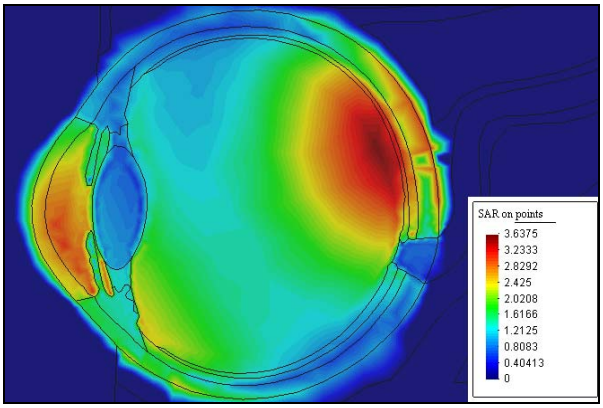

Fig. 12. SAR distribution [W/kg] inside the human eye caused by TM plane wave at frequency of 0.75 GHz.

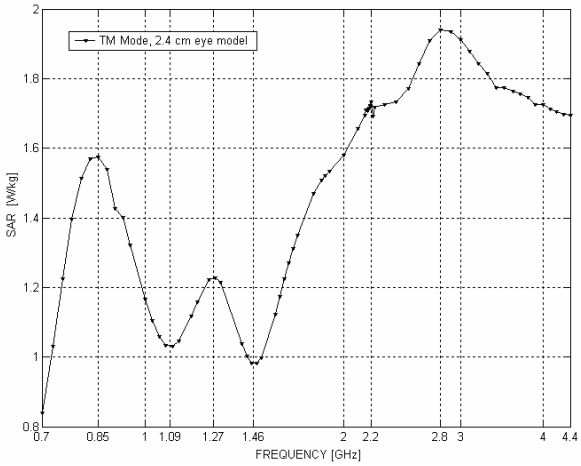

Fig. 13. Logarithmic plot of whole eye averaged SAR for TM mode plane wave in the frequency range of 0.7-4.4 GHz

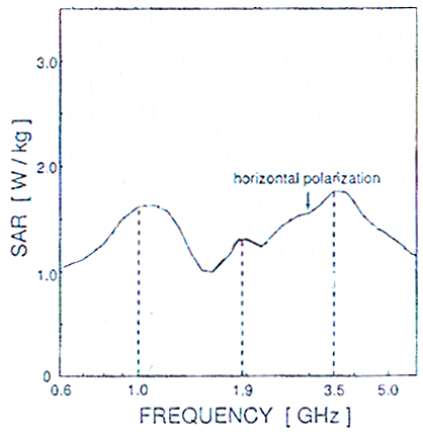

Fig. 14. Whole eye averaged SAR as calculated in ref. [16] by mean of the Finite Difference Time Domain (FDTD) method.

C. Temperature Rise in the Human Eye

The thermal properties used for temperature rise calculation are given in Table 1. Only the steady state temperature distribution has been considered, i.e. the temperature distribution at the moment in time when the thermal equilibrium is reached.

TABLE I
THERMAL PROPERTIES OF VARIOUS TISSUE TYPES COMPILED FROM REF. [16] USED IN TEMPERATURE RISE CALCULATION

Tissue type	*Mass Density* $\rho\left[\frac{kg}{m^3}\right]$	*Specific Heat* $C\left[\frac{J}{kg^\circ C}\right]$	*Thermal Conductivity* $k\left[\frac{J}{m\,s^\circ C}\right]$	*Blood Perfusion* $B\left[\frac{J}{m^3 s^\circ C}\right]$	*Metabolic Rate (Basal)* $Q_m\left[\frac{J}{m^3 s}\right]$
Lens	1100	3000	0.400	0	0
Cornea	1076	4178	0.580	0	0
Sclera	1170	4178	0.580	0	0
Nerve	1043	3600	0.503	35000	10000
Vitreous humor	1009	3997	0.594	0	0
Retina	1039	3680	0.565	35000	10000
Anterior chamber	1003	3997	0.578	0	0
Lens zonules	1040	3430	0.498	2700	690
Choroid	1060	3840	0.530	0	0
Cilliary muscle	1040	3430	0.498	2700	690
Brain grey matter	1039	3680	0.565	35000	10000
Bone	1810	1300	0.300	1000	0
Skin	1010	2500	0.420	9100	1000
Muscle	1040	3430	0.498	2700	690
Air	1.16	1300	0.025	0	0

Solution of the average and maximum thermal rise for plane wave power density of 5.0 mW/cm^2 is shown in Fig. 15 while the temperature rise in the eye over the frequency range from 0.7GHz to 4.4 GHz is shown in Fig. 16.

Surprisingly, the results reveal a peak of temperature rise at 0.85 GHz, this is near the frequency of 900 MHz which is widely used for the mobile communication technology. However, since the final results are significantly sensitive to geometrical variations of the model, we speculate that his peak may be shifted by different shapes of the eye, face and nose. Hence, more investigation in this direction is required.

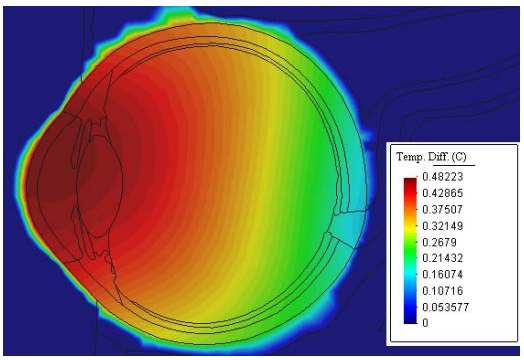

Fig.15. Temperature rise in the human eye due to the microwave heating. Incident plane wave is TM plane wave with frequency f=0.85 GHz. The power density of the plane wave is 5.0 mW/cm^2

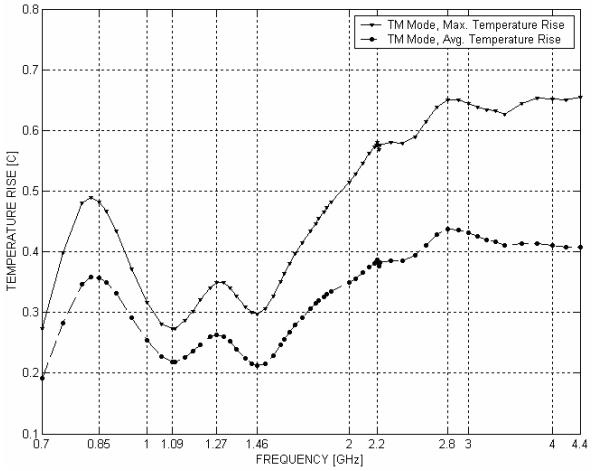

Fig. 16. Logarithmic plot of average and maximum temperature rise in the human eye. resulting from incident plane wave power density of 5.0 mW/cm^2

VI. CONCLUSION

Electromagnetic-thermal modeling of the human eye based on a new hybrid BEM/FEM method has been presented in the paper. This hybrid method has been chosen for the internal electric field calculation because it is well-suited for treating open boundary problems while allowing the scatterer to be inhomogeneous. The temperature response of the eye is obtained by solving the bio-heat transfer equation via standard finite element method. These methods may serve to evaluate the adverse effects of the EM fields on humans but it can serve for purpose of various medical treatments.

REFERENCES

[1] Akimasa Hirata, Toshiyuki Shiozawa: "Correlation of Maximum Temperature Increase and Peak SAR in the Human Head Due to Handset Antennas", IEEE Transactions on Microwave Theory and Techniques, Vol. 51, No. 7, July 2003, pp. 1834-1841

[2] Paolo Bernardi, Marta Cavagnaro, Stefano Pisa, Emanuele Piuzzi: "SAR Distribution and Temperature Increase in an Anatomical Model of the Human Eye Exposed to the Field Radiated by the User Antenna in a Wireless LAN", IEEE Transactions on Microwave Theory and Techniques, Vol. 46, No. 12, December 1998, pp. 2074-2082

[3] N. Siauve, R. Scoretti, N. Burais, L. Nicolas, A. Nicolas: "Electromagnetic fields and human body: a new challenge for electromagnetic field computation", COMPEL, Vol. 22, No. 3, 2003

[4] D.Poljak: "Human Exposure to Electromagnetic Fields", WIT Press, Southampton-Boston, 2003

[5] H.Dodig: "EM and Thermal Modeling of the Human Eye", MPhil Thesis, Wessex Institute of Technology, 2005

[6] D.Poljak and C.A. Brebbia: "Boundary Element Methods for Electrical Engineers", WIT Press, Southampton-Boston 2005.

[7] C.A.Brebbia and J.Dominguez: "Boundary Elements An Introductory Course", 2nd edition, Computational Mechanics Publications, Mc-Graw Hill Book Company, 1992

[8] D.Poljak, Choy Yoong Tham, Nikša Kovač: "The assesment of human exposure to low frequency and high frequency electromagnetic fields using boundary element analysis". Engineering Analysis with Boundary Elements 27 (2003)-10007

[9] D. Poljak, "Electromagnetic modelling of wire antenna structures". Southampton-Boston, WIT Press; 2002.

[10] Harry H. Pennes, "Analysis of Tissue and Arterial Blood Temperatures in the Resting Human Forearm", Journal of Applied Physiology, Vol. 1, No. 2, pp. 93-122,1948

[11] D.Poljak, N.Kovač: "The Electromagnetic-Thermal Analysis of Human Exposure to Radio Base Station Antennas", 17th International Conference on Applied Electromagnetics and Communications, ICECOM 2003, 1-3 Oct., 2005, Dubrovnik, Croatia

[12] P. Kolniko, D.R.Smith: "Numerical study of electromagnetic waves interacting with negative index materials", Department of Physics, University of California, San Diego

[13] United States National Library of Medicine, "The Visible Human Project", http://www.nlm.nih.gov/research/visible/visible_human.html

[14] K.S.Cole, Cole and R.H. Cole,"Dispersion and absorption in dielectrics: alternating current characteristics". Journal of Chemical Physics, Vol. 9, p. 341, 1941

[15] D.Andreucceti, R.Fossi, C. Petrucci, "Dielectric Properties of Body Tissues", Institute for Applied Physics, "Nello Carrara", Florence (Italy), [Online]. Available: http://niremf.iroe.fi.cnr.it/tissprop

[16] Akimasa Hirata, Shin-ichi Matsuyama, Toshiyuki Shiozawa,"Temperature Rises in the human Eye Exposed to EM Waves in the Frequency Range 0.6-6 GHz.", IEEE Transactions on Electromagnetic Compatibility, Vol. 42., No. 4, pp. 386-393, November 2000

Hrvoje Dodig received the graduate degree in applied electronics from the University of Split, Split, Croatia, in 2002 and the M.Sc. degree in from the University of Wales, Aberystwyth, U.K., in 2005. He is currently working toward the Ph.D. degree at Wessex Institute of Technology, Southampton, U.K. His MPhil thesis was in field of numerical modeling of the human eye and the work focused on hybrid BEM/FEM methods. Currently, his Ph. D. focuses on devising more accurate and practical hybrid BEM/FEM methods for solving electromagnetic influence on the human eye.

Andrés Peratta received the M.Sc. degree in physics from the University of Buenos Aires, Buenos Aires, Argentina, in 2001 and the Ph.D. degree from the University of Wales, Aberystwyth, U.K., in 2004. During 2005, he was a Postdoctoral Fellow and an Assistant Professor atWessex Institute of Technology (WIT), Southhampton, U.K., where he is currently the Head of the ICE Division. He is also a member of the Editorial Board of the *Journal of Communications, Software, and Systems*, which is sponsored by the IEEE. His current research interests include numerical modeling, boundary and finite element methods, electromagnetism, computational fluid dynamics, and continuum mechanics. Dr. Peratta is a member of the SoftCom Society and an ISAC member of the WIT International Conferences on Environmental Electromagnetic Compatibility, Simulation of Electrochemical Processes, and Computational Ballistics.

Dragan Poljak (M'96) received the B.Sc., M.Sc., and Ph.D. degrees in electrical engineering from the University of Split, Split, Croatia, in 1990, 1994, and 1996, respectively. He is a Full Professorwith the Department of Electronics, University of Split, and an Adjunct Professor atWessex Institute of Technology (WIT), Southampton, U.K. His current research interests include frequency and time domain computational methods in electromagnetics, particularly in the numerical modeling of wire antenna structures, and numerical modeling applied to the environmental aspects of electromagnetic fields. He is the author or coauthor of more than 180 journal and conference papers in the area of computational electromagnetics. He has also authored four books and one edited book. He is a member of the Editorial Board of the *Engineering Analysis with Boundary Elements* and the Editor of the WIT Press Series *Advances in Electrical Engineering and Electromagnetics*. Prof. Poljak is the recipient of the National Prize for Science. He is a Co-Chairman of the WIT International Conference on Computational Methods in Electrical Engineering and Electromagnetics and the International Conference on Environmental Electromagnetics.